Report

Current Biology

Early Jurassic origin of avian endothermy and thermophysiological diversity in dinosaurs

Graphical abstract

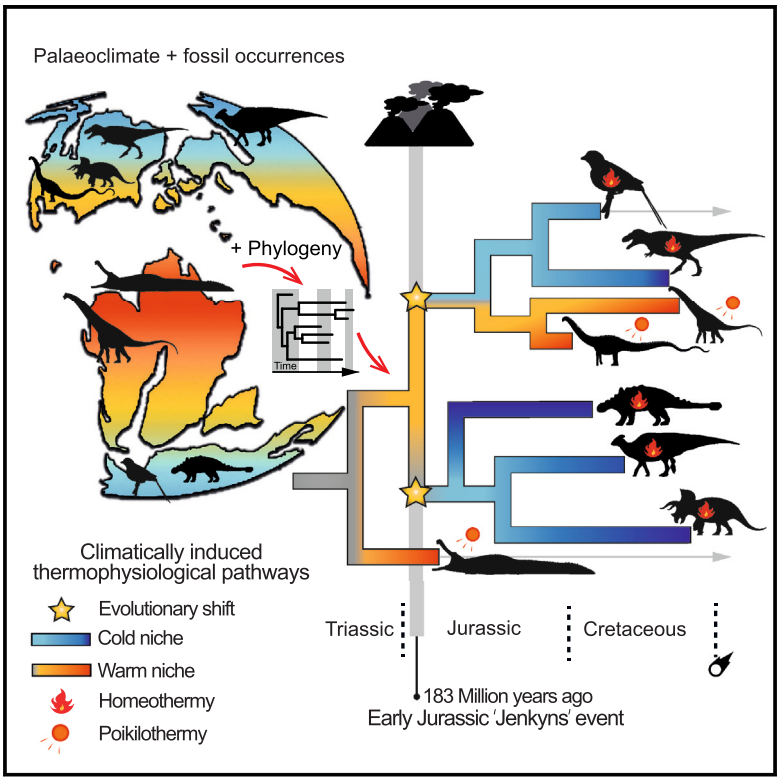

Highlights

- Warm-blooded dinosaurs flourished in varied climates
- Dinosaur groups adapted differently to climate, suggesting diverse thermophysiologies
- Endothermy in theropods and possibly ornithischians evolved by the Early Jurassic
- Sauropod niche conservatism suggests higher thermal sensitivity and poikilothermy

Authors

Alfio Alessandro Chiarenza, Juan L. Cantalapiedra, Lewis A. Jones, ..., Paul J. Valdes, Graciela Sotelo, Sara Varela

Correspondence

a.chiarenza15@gmail.com or alfio.chiarenza@ucl.ac.uk

In brief

Dinosaur acclimatization and the evolution of bird-like, independent thermoregulation are heavily debated. Chiarenza et al. quantify the evolution of dinosaur thermal strategies, showing trends toward cool niches ("warm-bloodedness") in ornithischians and theropods since the Early Jurassic and warmth conservatism ("cold-bloodedness") in sauropods.

Chiarenza et al., 2024, Current Biology *34*, 2517–2527
June 3, 2024
https://doi.org/10.1016/j.cub.2024.04.051

CellPress

Current Biology

CellPress
OPEN ACCESS

Report

Early Jurassic origin of avian endothermy and thermophysiological diversity in dinosaurs

Alfio Alessandro Chiarenza,[1,2,9,17,*] Juan L. Cantalapiedra,[3,4,5,11] Lewis A. Jones,[1,12] Sara Gamboa,[1,8,13] Sofía Galván,[1,14] Alexander J. Farnsworth,[6,7,15] Paul J. Valdes,[6,7] Graciela Sotelo,[1] and Sara Varela[1,10,16]

[1]Centro de Investigación Mariña, Departamento de Ecoloxía e Bioloxía Animal, Universidade de Vigo, Campus Lagoas-Marcosende, 36310 Vigo, Spain
[2]Department of Earth Sciences, University College London, Gower Place, London WC1E 6BS, UK
[3]Departamento de Paleobiología, Museo Nacional de Ciencias Naturales (CSIC), José Gutiérrez Abascal 2, 28006 Madrid, Spain
[4]GloCEE Global Change Ecology and Evolution Research Group, Departamento de Ciencias de la Vida, Universidad de Alcalá, 28801 Alcalá de Henares, Spain
[5]Museum für Naturkunde, Leibniz Institute for Evolution and Biodiversity Science, Invdralidenstraße 43, 10115 Berlin, Germany
[6]School of Geographical Sciences, University of Bristol, University Road, Bristol BS8 1SS, UK
[7]State Key Laboratory of Tibetan Plateau Earth System, Environment and Resources (TPESER), Institute of Tibetan Plateau Research, Chinese Academy of Sciences, Beijing 100101, China
[8]Universidad Complutense de Madrid, Av. Séneca 2, 28040 Madrid, Spain
[9]X (formerly Twitter): @AAlechiarenza
[10]X (formerly Twitter): @MapasLab
[11]X (formerly Twitter): @singerstone
[12]X (formerly Twitter): @LewisAlanJones
[13]X (formerly Twitter): @Paleobicha
[14]X (formerly Twitter): @sofiaGA96
[15]X (formerly Twitter): @Climate_AlexF
[16]X (formerly Twitter): @_Sara_Varela
[17]Lead contact
*Correspondence: a.chiarenza15@gmail.com or alfio.chiarenza@ucl.ac.uk
https://doi.org/10.1016/j.cub.2024.04.051

SUMMARY

A fundamental question in dinosaur evolution is how they adapted to long-term climatic shifts during the Mesozoic and when they developed environmentally independent, avian-style acclimatization, becoming endothermic.[1,2] The ability of warm-blooded dinosaurs to flourish in harsher environments, including cold, high-latitude regions,[3,4] raises intriguing questions about the origins of key innovations shared with modern birds,[5,6] indicating that the development of homeothermy (keeping constant body temperature) and endothermy (generating body heat) played a crucial role in their ecological diversification.[7] Despite substantial evidence across scientific disciplines (anatomy,[8] reproduction,[9] energetics,[10] biomechanics,[10] osteohistology,[11] palaeobiogeography,[12] geochemistry,[13,14] and soft tissues[15–17]), a consensus on dinosaur thermophysiology remains elusive.[1,12,15,17–19] Differential thermophysiological strategies among terrestrial tetrapods allow endotherms (birds and mammals) to expand their latitudinal range (from the tropics to polar regions), owing to their reduced reliance on environmental temperature.[20] By contrast, most reptilian lineages (squamates, turtles, and crocodilians) and amphibians are predominantly constrained by temperature in regions closer to the tropics.[21] Determining when this macroecological pattern emerged in the avian lineage relies heavily on identifying the origin of these key physiological traits. Combining fossils with macroevolutionary and palaeoclimatic models, we unveil distinct evolutionary pathways in the main dinosaur lineages: ornithischians and theropods diversified across broader climatic landscapes, trending toward cooler niches. An Early Jurassic shift to colder climates in Theropoda suggests an early adoption of endothermy. Conversely, sauropodomorphs exhibited prolonged climatic conservatism associated with higher thermal conditions, emphasizing temperature, rather than plant productivity, as the primary driver of this pattern, suggesting poikilothermy with a stronger dependence on higher temperatures in sauropods.

RESULTS

Tempo and mode in dinosaurian climatic niche evolution

Dinosauria was conventionally regarded as a group of stereotypically lumbering, slow-moving reptiles, sharing characteristics with most ectothermic and poikilothermic vertebrates—that is, species with higher variation in internal temperature that rely on environmental heat for homeostasis.[2] However, recent discoveries culminating two centuries of research[4,22] are challenging this "cold-blooded," environmentally regulated body

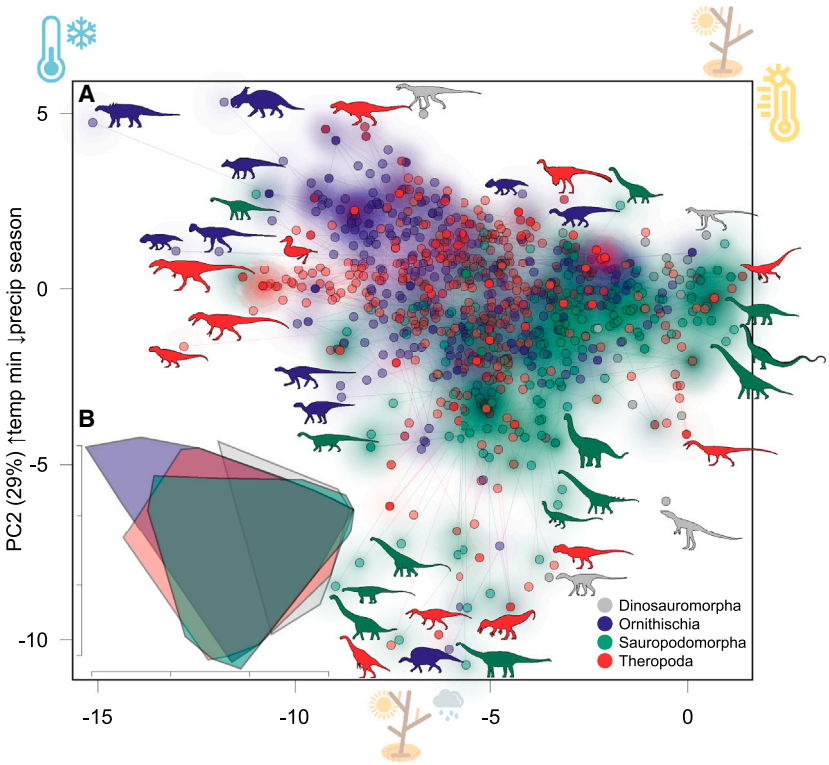

Figure 1. Phylogenetic-climatic niche space for Mesozoic dinosaurs

(A) A phylogenetic principal-component analysis (PCA) represents the projection of the Dinosauria supertree (STAR Methods) into a PCA of climatic variables. PC1 axis shows strong positive correlation with maximum temperature (↑temp max), low positive correlation with precipitation seasonality (↕precip season), strong negative correlation with minimum temperature (↓temp min), and strong negative correlation with minimum precipitation (↓precip min). PC2 axis shows strong positive correlation with minimum temperature (↑temp min) and negative correlation with precipitation seasonality (↓precip season). Shadows around points highlight the relative density in the principal component space of non-dinosaurian Dinosauromorpha (gray), Ornithischia (blue), Sauropodomorpha (green), and Theropoda (red).

(B) Lower left plot shows 95% confidence interval convex hulls for each dinosauromorph subclade. Blue thermometer (top left corner) symbolizes the direction of the vector in the PC space region for cold temperatures; yellow thermometer (top right corner) indicates the direction of the vector in PC space for warm temperatures; brown shrub (top right corner) depicts dry conditions, while the same with a gray, rainy cloud (mid, lower side of the graph) illustrates seasonal conditions.

Silhouettes represent the following taxa (clockwise from the higher left corner): *Minmi*, *Edmontosaurus*, *Pachyrhinosaurus*, *Tyrannosaurus*, *Asilisaurus*, *Gracilicratops*, *Harpymimus*, *Altirhinus*, *Gobititan*, *Suzhousaurus*, *Marasuchus*, *Pampadromaeus*, *Herrerasaurus*, *Vulcanodon*, *Diplodocus*, *Giraffatitan*, *Coelophysis*, *Dromomeron*, *Gondwanatitan*, *Tapuiasaurus*, *Anchisaurus*, *Siamotyrannus*, *Diodorus*, *Suchomimus*, *Phuwiangosaurus*, *Ouranosaurus*, *Irritator*, *Tangvayosaurus*, *Nanshiungosaurus*, *Aeolosaurus*, *Rebbachisaurus*, *Chuxiongosaurus*, *Tethyshadros*, *Koreanosaurus*. *Genyodectes*, *Mapusaurus*, *Vegavis*, *Goyocephale*, and *Rhoetosaurus*.

See also repository data file 1.

temperature paradigm, painting a more nuanced picture. It highlights the emergence—at least within certain dinosaurian lineages (e.g., Maniraptora)—of traits typical of endothermic, homeothermic, and tachymetabolic (highly active) tetrapods capable of maintaining a constant body temperature through internally generated heat.[23]

We use a phylogenetic comparative method framework to explicitly integrate concepts of tempo and mode from established macroevolutionary theory in vertebrate paleontology.[24,25] This approach quantitatively explores evolutionary patterns signaling likely shifts in thermophysiology due to the invasion into novel adaptive landscapes (*sensu* Simpson[24]) and specifically in terms of climatic tolerance. Through the application of phylogenetic comparative methods and global palaeoclimate modeling,[26] including climatically calibrated dinosaur phylogenies analyzed through a set of evolutionary models,[27–29] we reconstructed the climatic adaptive landscape[30] of Dinosauria throughout the Mesozoic. We tested three hypothetical scenarios for the evolution of the dinosaurian climatic niche landscape: (1) relaxed plasticity (RP), involving a continuous invasion of new climatic niches without directional limitations imposed by physical factors; (2) the influence of internal (phylogenetic or clade-dependent) constraints (IC); and (3) the impact of external (climatic regime shifts) constraints (EC) at specific time horizons. Evolution shaped by external pressures may have influenced climatic occupation in the adaptive landscape, prompting biotic adaptations in terms of thermophysiological plasticity or the differential success of climatically more adaptive lineages. Additionally, we examined how biome occupation during the Mesozoic influenced the exploitation of dinosaur-suitable climates. Our study directly assessed the timing and modes of transitions to different climatic niches in dinosaur evolution, allowing us to infer distinct thermophysiological strategies within different Dinosauria subclades.

The occupation of climatic niche space throughout the Mesozoic

The evolution of dinosaurian climatic niches followed two main dimensions (Figure 1): one (principal component 1, PC1) controlled by a combination of maximum and minimum temperatures, minimum precipitation, and precipitation seasonality and the other (PC2) by minimum temperature and precipitation seasonality. Dinosauromorphs started diversifying in dry environments characterized by high temperatures (Figure 1A). From these arid conditions, sauropodomorphs initially invaded broader niche dimensions, with some early diverging outliers occupying relatively cooler conditions (e.g., *Plateosauravus*, *Antetronitus*, and *Rhoetosaurus*), then primarily expanded throughout drier and warmer niches, stalling at high temperatures but shifting toward more seasonal precipitation conditions

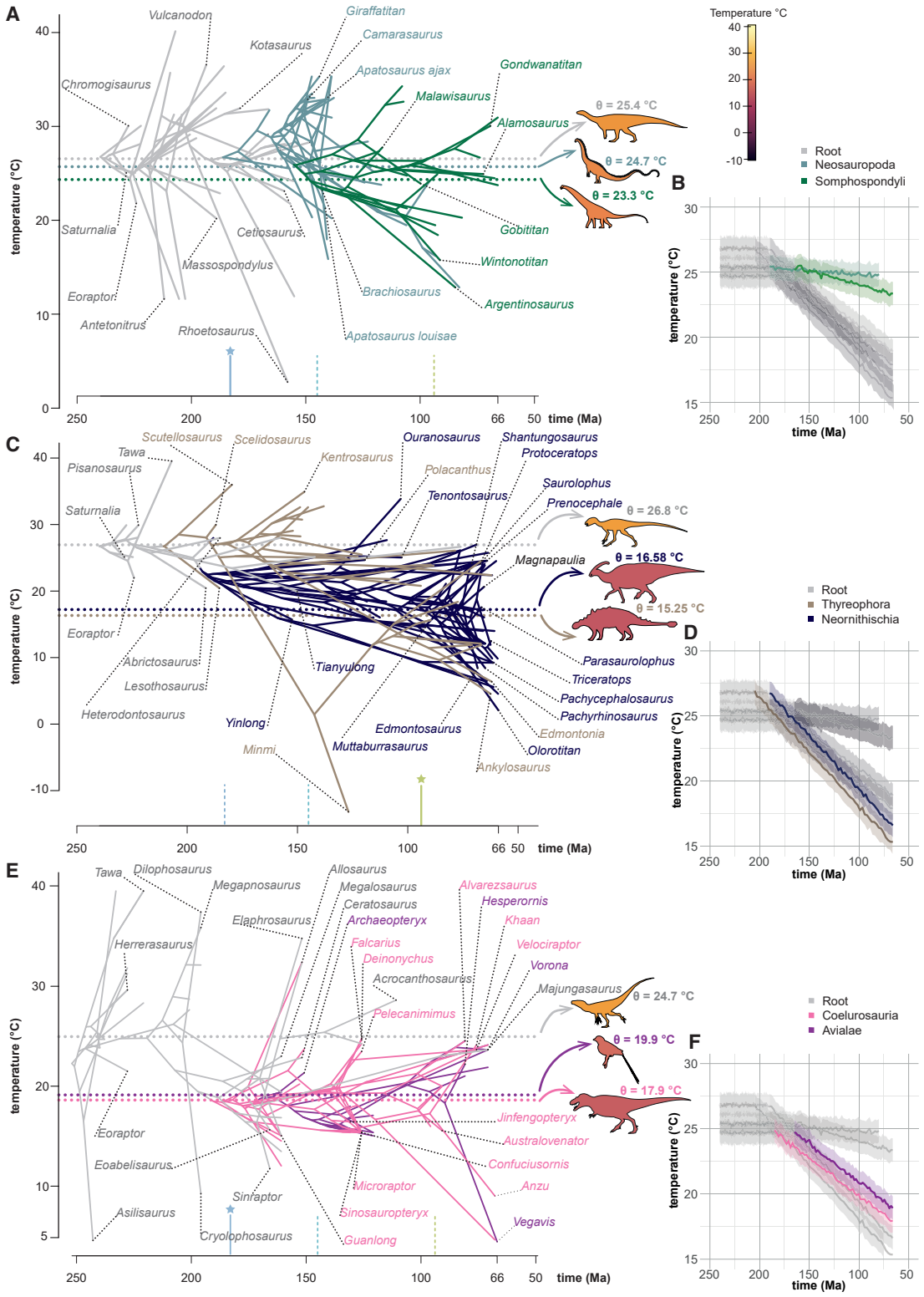

Figure 2. Macroevolutionary climatic landscape in Dinosauria throughout the Mesozoic

Evolutionary regimes along the temperature axis (in °C) are shown for Sauropodomorpha (A and B), Ornithischia (C and D), and Theropoda (E and F). Clade partitions along the trees (A, C, and E) are portrayed in different colors with horizontal dotted lines showing optima (θ) for each clade partitions. Trends in temperature optima occupation are simplified in (B), (D), and (F). Dinosaur silhouettes colors change according to the temperature at each θ. Stars on top of vertical bars indicate significant (following model choice according to AIC values; STAR Methods; Table S1) changes in time-dependent partitions across the

(legend continued on next page)

in later diverging groups. Ornithischians followed cooler and wetter environments through their evolution, with theropods tracking the other two dinosaur subclades. Although both theropods and ornithischians evolved toward lower temperatures (Figure 1B), Ornithischia exhibited a more pronounced preference for cooler conditions, especially in later thyreophorans, ceratopsians, and hadrosaurids. Earlier diverging neornithischians occupied warmer and more seasonal conditions, closer to their dinosauromorph relatives. Theropods displayed a wide climatic niche, largely overlapping with the composite ornithischian and sauropodomorph climatic space. They invaded colder, yet slightly more seasonal, precipitation conditions in later diverging carnosaurs and coelurosaurs (including avialians), while still maintaining ancestrally warmer and drier niches in some members of all these clades. Although theropods occupy a broad climatic space, they tend to more densely occupy a cooler climatic space later in their evolution. Overall, ornithischians and theropods increased their climatic niche disparity compared with sauropodomorphs and ancestral dinosauromorphs. Ornithischia and Theropoda were both projected toward cooler niches, with a preference for more humid conditions in the former and higher seasonality (in terms of humidity) in the latter (Figure 1B).

Macroevolution of the climatic adaptive landscape in Dinosauria

The climatic niche evolution of Mesozoic dinosaurs is expressed differentially among the main subclades of Dinosauria (Figure 2). Sauropodomorphs are restricted to higher temperatures (23.3°C–25.4°C), while ornithischians and theropods exhibit broader thermal ranges. Overall, we find that no single regime model comprehensively explains the thermal evolution of each subclade. Instead, Ornstein-Uhlenbeck models of evolution (OUMA and OUMVA) are favored (Table S1; repository data file 3), suggesting that climatic niche exploration is influenced by physically constrained models following distinct macroevolutionary thermal optima (θ). For sauropodomorphs (Figure 2), model-fit results indicate a conservative evolution from an ancestral temperature of 25.4°C, with a root evolutionary rate (σ^2) of 1.85×10^{-5} and an attraction value (α) of 0.6×10^{-1}. Different subclades within Sauropodomorpha reached distinct but close thermal optima, with Neosauropoda reaching θ = 24.7°C (Figure 2A), exhibiting comparable attraction values ($\alpha = 0.7 \times 10^{-1}$) to the root but slower rates (σ^2) of 3.2×10^{-6}. Somphospondyli (later diverging titanosaurs) reach a temperature optimum of θ = 23.3°C (Figure 2A) with an increased rate ($\sigma^2 = 1.2 \times 10^{-5}$) and consistent attraction value ($\alpha = 0.6 \times 10^{-1}$). A significant transition (Table S1) occurs during the "Jenkyns" early Toarcian oceanic anoxic event (OAE), with a rate increase from $\sigma^2 = 0.26 \times 10^{-6}$ to $\sigma^2 = 0.13 \times 10^{-3}$ with almost equivalent attraction ($\alpha_{1-2} = 0.91 \times 10^{-1}$–$0.69 \times 10^{-1}$) for a temperature decrease from the root state (z_0) of 28.1°C to a later optimum of θ = 23.4°C (Figure 2A).

Ornithischia undergoes a rapid transition ($\sigma^2 = 0.59 \times 10^{-7}$ to $\sigma^2 = 0.14 \times 10^{-4}$) from warm climatic niches starting at z_0 = 26.8°C in the Early Jurassic to cooler climatic niches in Thyreophora, reaching θ = 15.25°C, accompanied by reduced attraction values ($\alpha = 1.5 \times 10^{-2}$; Figures 2C and 2D). Neornithischia (Figure 2C) shows a slowed rate ($\sigma^2 = 0.54 \times 10^{-5}$) and an attraction to cooler niches (θ = 16.58°C, $\alpha = 3.7 \times 10^{-2}$). The regime transition is sub-optimally modeled to occur (Table S1) at the Cenomanian/Turonian (C/T) boundary (Figure 2C), with negligibly different attraction values ($\alpha_{1-2} = 0.4 \times 10^{-1}$ to 0.3×10^{-1}) from pre-C/T values. The favored clade-partitioned model has equal attraction and rate values (OUMA), depicting a transition from z_0 = 26.8°C to θ = 15.25°C in Thyreophora and θ = 16.58°C in Neornithischia (Figure 2C).

Theropods (Figures 2E and 2F) exhibit an abrupt decrease in temperature optima favored in the model partitioned between their root, Coelurosauria, and Avialae, compared with the stepwise pattern when partitions are modeled at the base of the dinosauromorph node, at the base of Theropoda, and in Coelurosauria. This model displays a decrease in rates ($\sigma^2 = 0.1 \times 10^{-4}$ to $\sigma^2 = 0.3 \times 10^{-6}$) with a slight increase in attraction values ($\alpha_{1-2} = 0.37 \times 10^{-1}$ to 0.64×10^{-1}), from the root temperature of z_0 = 24.7°C to a lower optimum of θ = 19.9°C in Coelurosauria. Avialae (Figure 2E) experiences an accelerated rate ($\sigma^2 = 0.5 \times 10^{-4}$) with a slight decrease in attraction values (α = 0.25), resulting in a temperature optimum of θ = 17.9°C. The "Jenkyns event" (Figure 2E) plays a pivotal role in partition transitions (Table S1), influencing changes in rates ($\sigma^2 = 0.45 \times 10^{-4}$ to $\sigma^2 = 0.2 \times 10^{-6}$), attraction values ($\alpha_{1-2} = 0.13 \times 10^{-1}$ to 0.19×10^{-1}), and cooling in temperature optima from z_0 = 28.03 °C to θ = 18.82 °C.

Testing dinosaurian occupation of climatic zones due to biome preferences

Sauropodomorph preferences for warm environments (thermal bound hypothesis, TBH) might be seen as a secondary result of their large size or a sampling bias. Large terrestrial primary consumers preferentially inhabit regions of elevated productivity,[31] so they may have favored lower latitudes (the productivity bound hypothesis, PBH). Although previous studies have quantified the relative sampling control for latitude and the quality of the fossil record,[12,32] there is currently a lack of quantification on whether Jurassic-Cretaceous sauropods were restricted to low latitude due to their selective or exclusive occupancy of tropical, highly productive biomes. To test these hypotheses (i.e., linking sauropodomorph distribution to biomes), we plotted the taxa used in our phylogenetic modeling analyses on palaeogeographic maps (repository data file 4) of broad climatic zones according to an adapted Köppen scheme.[33,34] Recognizing the substantial influence of largely unknown factors (such as substrate lithology and taxonomic composition of vegetation) during the Mesozoic, we opted for climatic zones[35] over strict biomes, with the assumption that climatic zones could effectively serve

Jenkyns event (~183 Ma), the Jurassic/Cretaceous (~145 Ma), and the Cenomanian/Turonian (93.9 Ma) boundaries (with dotted lines showing non-significant trend variations).
Silhouettes (top to bottom) represent the following taxa: *Plateosaurus*, *Diplodocus*, *Alamosaurus*, *Heterodontosaurus*, *Euoplocephalus*, *Parasaurolophus*, *Herrerasaurus*, *Protopteryx*, and *Gorgosaurus*.
See also Table S1 and repository data files 2 and 3.

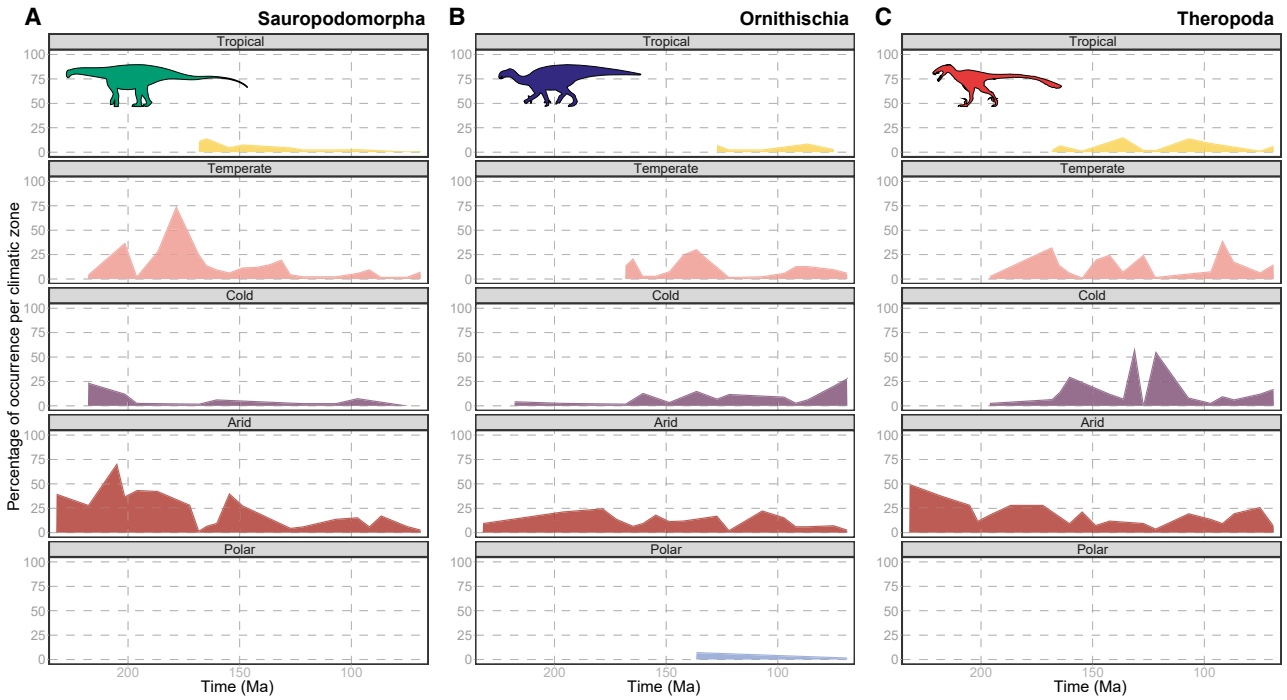

Figure 3. Dinosaur abundance in climatic zones

Taxic-occurrence quantification as percentage of total occurrences per time bin for Sauropodomorpha (A), Ornithischia (B), and Theropoda (C) in which the highest productive climatic zones are arranged on top and less productive ones at the bottom. Time bins with missing data are represented by interpolated values between time bins.

Silhouettes (left to right) represent the following taxa: *Nigersaurus*, *Iguanodon*, and *Deinonychus*.

See also repository data file 4.

as proxies for the latter. Sauropodomorphs (Figure 3A) are equally prevalent in tropical, temperate, and arid regions, compared with cold and temperate zones, and are absent in polar regions. Contrary to the expectation of the PBH, sauropodomorphs are comparatively less represented in tropical regions than ornithischians and theropods, having a higher prevalence in low-productivity arid regions, particularly during the Late Jurassic–Early Cretaceous interval. By contrast, Ornithischia, which are highly abundant in tropical zones, are equally diverse in cold and polar zones.

These observations are consilient with the fossil record of sauropod-rich areas such as the semi-arid and seasonal Late Jurassic Morrison Formation[12,36] and the arid to seasonal palaeoenvironment of the Late Cretaceous Huincul Formation in Argentina,[37] both sauropod-bearing units yielding some of the largest representative of this clade. These formations have been generated in warm, xeric to seasonal palaeoenvironments, conditions preferentially suitable for sauropods,[12] an observation withstanding potential sampling biases.[12,38,39] Furthermore, high latitudes remained highly productive areas in the Mesozoic,[40,41] particularly in the Cretaceous, when pinoid conifers dominated mid-to-high latitudes.[42] Forested covers thrived in the poles during the Mesozoic (based on evidence from Antarctica and Alaska, especially in Late Cretaceous deposits[42–45]), hardly exerting a productivity-dependent constraint on dinosaurian primary consumers, as also evidenced by the high-latitude occupation and sustained polar diversity of ornithischian dinosaurs (Figure 3B).

High-latitude dispersal routes would have still been viable to sauropods,[46] as invoked for Lower Cretaceous titanosaurs[47,48]: although these taxa have been suggested to co-occur in relatively cold palaeoenvironments, due to the generally warmer Early Cretaceous climate, these localities (repository data file 1) are characterized by mean annual temperatures above freezing levels (~10°C–15°C) as also supported by palaeobotanical evidence of temperate rainforests.[49] High-latitude regions may have been thermally challenging for sauropods, but an alternative hypothesis is that sauropods, although physiologically capable of surviving in high-latitude environments, might have been less adapted to do so than other dinosaurs. Competition with ornithopods and ceratopsians in the Northern Hemisphere could have led to competitive exclusion on a large scale, resulting in sauropod absence from high-latitude faunas. Conversely, the scarcity of ceratopsians in the Southern Hemisphere and the late arrival of hadrosaurids might have allowed sauropods to persist longer in the Southern Hemisphere.[12]

DISCUSSION

Dinosaur diversification throughout the climatic adaptive landscape

Early dinosauromorphs appeared and diversified in dry and hot environments (Figure 1), while later diverging subclades evolved toward broader niche dimensions, reflecting different climatic preferences and potential thermophysiological constraints.

Sauropodomorphs favored high temperatures, while ornithischians and theropods explored a broader range of thermal landscapes in their evolutionary histories. This divergence in climatic niches likely played a crucial role in shaping the ecological diversity, biogeographic history, and success of these groups.[4,12,46,50]

The preference for cooler and wetter conditions within ornithischians, particularly in later thyreophorans, ceratopsians, and hadrosaurids, suggests a trend toward increased humidity and seasonality in their habitats. This adaptation may have facilitated their continuous persistence at high latitudes and occupation of broader climatic zones (Figure 3B), ranging from tropical to polar environments.[4,12,51] Theropods also displayed a wide range of climatic preferences, with some taxa retaining ancestrally warmer and drier niches, while others adapted to cooler and slightly more seasonal conditions. The temporal-shift phylogenetic models suggest a possible transition toward broader thermal diffusion since the late Early Jurassic Jenkyns event, a time likely associated with the radiation of the main tetanuran clades,[52] and possibly early pannaraptorans.[53–55] Key changes in climatic preferences during specific geological events, such as the Jenkyns and the Cretaceous Thermal Maximum,[56] indicate critical periods of adaptation coinciding with hyperthermals.[57] The Jenkyns event, associated with the Early Toarcian OAE, imposed macroevolutionary EC, significantly influencing temperature optima shifts in sauropodomorphs and theropods. Recent empirical evidence[58] suggests that eusauropod sauropodomorphs attained large sizes (>10 m in length) and radiated around this time horizon (184–180 Ma), coinciding with a short-lived episode of global warming, marine anoxia, and a large-scale magmatic event. Concurrent climatic perturbations marked a drastic decrease in floral diversity, as documented by the contemporaneous rise of conifers. This episode might have strongly affected clades of terrestrial animals attaining gigantic size at the time,[58,59] potentially driving the explosion in the diversification of the main dinosaurian clades.[57]

The exploration of thermal niches during this pivotal transition may have been crucial to dinosaurian success thereafter, due to the consequent ecosystem reorganization and increase in bioregional suitability for the thermically unconstrained ornithischians and theropods.[12] Once the likely more eurythermal (thermally more adaptable) and widely distributed non-eusauropod sauropodomorphs declined,[7,60] the thermophilic eusauropods colonized more tropical latitudes and southern continents.[12,50] Our interpretations reconstruct an early selection of genasaurian (Neornithischia+Thyreophora) ornithischians of cooler niches (mostly dominated by IC throughout their macroevolutionary history), with a stronger temporal signal (EC) later, at the C/T boundary (C/T, 93.9 Ma). The early invasion of cool niches by thyreophorans and neornithischians aligns with the current mosaic of morphological traits (from integument[61] to ventilation[62,63]), suggesting an early attainment of a homeothermic (possibly endothermic) physiology in these clades, enabling them to colonize and persist in even extreme latitudes since the Early Jurassic. The pronounced shift (EC) in ornithischian optimal climate at the C/T boundary, coincides with a hyperthermal event known as the Cretaceous Thermal Maximum.[56] This event aligns with documented eustatic and atmospheric changes that may have influenced palaeodiversity and faunal biogeography.[64,65] This transition from the Early to Late Cretaceous witnessed the evolutionary appearance and radiation of Hadrosauridae,[66,67] highly represented in our dataset. The extent to which the thermal upheaval directly influenced ornithischians (and dinosaurs as a whole) or if the subsequent floral and broader biotic changes had a stronger impact should be the focus of more detailed studies across the C/T.

Ornithischians (at least ancestrally) and theropods, in which protofeathered integument structures or other osteological adaptations potentially linked to homeothermy and higher energetic needs have been found,[16,62,63] demonstrate remarkable adaptability across varied climatic zones. On the other hand, the more thermophilic sauropodomorphs show a specialized preference for low latitudes[12,46] and heating sources.[68] Given the broad ecomorphological diversification of Dinosauria, it is unlikely that any single anatomical or ecological factors (body size, integument, and dietary preferences) acted as major drivers of the macroevolutionary patterns reported here. Yet thermophysiology likely had an intricate role in relation to the evolution of several other ecomorphologies. For example, the lower body-size niches occupied by ornithischians in comparison with sauropods might be partially explained by the macroevolutionary saturations the latter exerted on large-size niches. Gigantothermy might have been adaptive for sauropod poikilothermy (e.g., to maintain a more active level at lower metabolic costs during extended foraging times). Large sauropods were likely more efficient at accumulating and dissipating heat[69,70] due to their unique bauplan.[71] This might have led to a further relaxation of their macroevolutionary trends stabilizing at higher thermal optima after an early, active invasion of this high-temperature niche space[60] matching with the evolution of giant body sizes (with few outliers below 1,000 kg and later body-size selective regimes around 15,000–17,000 kg[72]).

Notably, these results provide novel insights into the origin of avian endothermy, suggesting that this evolutionary trajectory within theropods toward thermal niche relaxation likely started in the latest Early Jurassic (Figure 2C), a crucial period for the radiation of coelurosaurs and possibly early diverging avian clades.[55,73,74] The attainment of endothermy could have been exaptive[75] in surviving environmental stressors like those imposed by the Jenkyns event. Early life history with longer developmental times in early theropods[76] and faster growth rates in later taxa represents a potential adaptive trait that emerged from this Early Jurassic transition. As such, endothermy may represent an evolutionary by-product of a life-history phenomenon with an ecologically selected process.[77] Furthermore, the attainment of endothermy could have fueled the emergence of entire lineages. Early diverging small,[53] feathered, homeothermic (and potentially endothermic) coelurosaurs might have been successfully selected to fill a cooler spectrum of the theropod climatic landscape, unfolding at broader thermal niches in later radiations. Although this process might have ensured a heterogeneous diversification of body sizes and ecologies, it might have set up the macroevolutionary and macroecological scenario for the radiation of highly active, high-energy demanding Avialae. Noteworthy, this process probably happened during a relatively obscure time in dinosaur evolutionary history[55] (the relatively poorly sampled Early-Middle Jurassic transition[78]), which matches with the radiation of the

main clades of theropods,[52] generating an interesting prediction for future directed sampling in this time horizon.

These findings highlight a potential link between climatic dynamics and the early development of endothermic traits, offering clues to the origin of birds and the heterogeneous thermophysiological strategies adopted by Mesozoic dinosaurs, contributing to a more nuanced understanding of dinosaurian evolution and the interplay between climate and ecological diversity.

STAR★METHODS

Detailed methods are provided in the online version of this paper and include the following:

- KEY RESOURCES TABLE
- RESOURCE AVAILABILITY
  - Lead contact
  - Materials availability
  - Data and code availability
- EXPERIMENTAL MODEL AND SUBJECT DETAILS
  - Fossil dataset
  - Phylogenetic Data for macroevolutionary modelling
  - Palaeoclimate model
- METHOD DETAILS
  - Phylogenetic Principal Component Analyses
  - Ancestral State Reconstruction
  - Macroevolutionary OU modelling
  - Climatic zones
- QUANTIFICATION AND STATISTICAL ANALYSIS
  - Phylogenetic comparative model performance evaluation

SUPPLEMENTAL INFORMATION

Supplemental information can be found online at https://doi.org/10.1016/j.cub.2024.04.051.

ACKNOWLEDGMENTS

We thank Phil Mannion (UCL) for discussions on sauropod palaeobiology, Oliver Rauhut (LMU) for discussions on theropod phylogenies, Matthew Carrano (SNMNH) for discussion and insights regarding herbivore dinosaur distribution and macroecology, Pavel Skutschas (SPBU) and Tony Fiorillo (NMMNH) for discussions on the Siberian and polar fossil record, and the editor (Florian Maderspacher) and four anonymous reviewers for their insightful comments, which greatly improved the quality of this paper. This is Paleobiology Database publication number 486. All silhouettes throughout this paper are sourced from http://phylopic.org/ and are licensed under Creative Commons licenses: CC BY 3.0 (https://creativecommons.org/licenses/by/3.0/), CC BY-SA.3.0 (https://creativecommons.org/licenses/by-sa/3.0/), and CC BY-NC-SA.3.0 (https://creativecommons.org/licenses/by-nc-sa/3.0/). Their creators (Pete Buchholz, Manuel Brea Lueiro, Matt Dempsey, Roberto Diaz Sibaja, based on Domser, DiBgd, Tasman Dixon, Andrew A. Farke, Scott Hartman, Jaime Headden, Ivan Iofrida, Jagged Fang Designs, T. Michael Keesey, Martin Kevil, Andrew Knight, Matt Martyniuk, Gareth Monger, Bruno Navarro, Diego Ortega, Remes K, Ortega F, Fierro I, Joger U, Kosma R, et al., Iain Reid, Nobu Tamura, Mathew Wedel) are acknowledged. S.V., A.A.C., L.A.J., G.S., S. Gamboa, and S. Galván were supported through a European Research Council (ERC) starting grant under the European Union's Horizon 2020 Research and Innovation Programme (grant no. 947921). A.A.C. was also supported through a Juan de la Cierva-formación 2020 fellowship (FJC2020-044836-I) funded by the Ministry of Science and Innovation from the European Union Next Generation EU/PRTR and partially funded by a Royal Society Newton International Fellowship (NIF\R1\231802). J.L.C. was funded by the Talent Attraction Program of the Madrid Government and the Universidad de Alcalá (2017-T1/AMB5298). L.A.J. was also supported by a Juan de la Cierva-formación 2021 fellowship (FJC2021-046695-I) funded by the Ministry of Science and Innovation from the European Union Next Generation EU/PRTR. S. Gamboa was also funded by the Ministry of Universities and the Next Generation European Union programme through a Margarita Salas grant from Universidad Complutense de Madrid (CT31/21). S. Galván was also funded by a predoctoral fellowship from Universidade de Vigo (PREUVIGO-2022). A.J.F. and P.J.V. acknowledge NERC grants NE/X018253/1, NE/X015505/1, NE/V011405/1, and NE/X013111/1. A.F. acknowledges the Chinese Academy of Sciences Visiting Professorship for Senior International Scientists (2021FSE0001).

AUTHOR CONTRIBUTIONS

Conceptualization, A.A.C.; methodology, A.A.C., J.L.C., A.J.F., and P.J.V.; GCM simulations, P.J.V. and A.J.F.; investigation, A.A.C., J.L.C., L.A.J., A.J.F., S. Gamboa, and S. Galván; visualization, A.A.C., S. Gamboa, S. Galván, and A.J.F.; supervision, A.A.C. and S.V.; writing – original draft, A.A.C.; writing – review & editing, all authors.

DECLARATION OF INTERESTS

The authors declare no competing interests.

Received: February 7, 2024
Revised: March 25, 2024
Accepted: April 22, 2024
Published: May 15, 2024

REFERENCES

1. Roger, T.D.K., and Olson, E.C. (1980). A Cold Look at the Warm-Blooded Dinosaurs (Westview Press for the American Association for the Advancement of Science).
2. Bakker, R.T. (1972). Anatomical and ecological evidence of endothermy in dinosaurs. Nature *238*, 81–85. https://doi.org/10.1038/238081a0.
3. Chiarenza, A.A., Fiorillo, A.R., Tykoski, R.S., McCarthy, P.J., Flaig, P.P., and Contreras, D.L. (2020). The first juvenile dromaeosaurid (Dinosauria: Theropoda) from Arctic Alaska. PLOS ONE *15*, e0235078. https://doi.org/10.1371/journal.pone.0235078.
4. Druckenmiller, P.S., Erickson, G.M., Brinkman, D., Brown, C.M., and Eberle, J.J. (2021). Nesting at extreme polar latitudes by non-avian dinosaurs. Curr. Biol. *31*, 3469–3478.e5. https://doi.org/10.1016/j.cub.2021.05.041.
5. Ostrom, J.H. (1969). Osteology of *Deinonychus antirrhopus*, an Unusual Theropod from the Lower Cretaceous of Montana (Yale University Press). https://doi.org/10.2307/j.ctvqc6gzx.
6. Brusatte, S.L., O'Connor, J.K., and Jarvis, E.D. (2015). The origin and diversification of birds. Curr. Biol. *25*, R888–R898. https://doi.org/10.1016/j.cub.2015.08.003.
7. Olsen, P., Sha, J., Fang, Y., Chang, C., Whiteside, J.H., Kinney, S., Sues, H.-D., Kent, D., Schaller, M., and Vajda, V. (2022). Arctic ice and the ecological rise of the dinosaurs. Sci. Adv. *8*, eabo6342. https://doi.org/10.1126/sciadv.abo6342.
8. Codd, J.R., Manning, P.L., Norell, M.A., and Perry, S.F. (2008). Avian-like breathing mechanics in maniraptoran dinosaurs. Proc. Biol. Sci. *275*, 157–161. https://doi.org/10.1098/rspb.2007.1233.
9. Tanaka, K., Zelenitsky, D.K., Therrien, F., and Kobayashi, Y. (2018). Nest substrate reflects incubation style in extant archosaurs with implications for dinosaur nesting habits. Sci. Rep. *8*, 3170. https://doi.org/10.1038/s41598-018-21386-x.
10. Clarke, A. (2013). Dinosaur energetics: setting the bounds on feasible physiologies and ecologies. Am. Nat. *182*, 283–297. https://doi.org/10.1086/671259.
11. Bailleul, A.M., O'Connor, J., and Schweitzer, M.H. (2019). Dinosaur paleohistology: review, trends and new avenues of investigation. PeerJ *7*, e7764. https://doi.org/10.7717/peerj.7764.

12. Chiarenza, A.A., Mannion, P.D., Farnsworth, A., Carrano, M.T., and Varela, S. (2022). Climatic constraints on the biogeographic history of Mesozoic dinosaurs. Curr. Biol. *32*, 570–585.e3. https://doi.org/10.1016/j.cub.2021.11.061.

13. Dawson, R.R., Field, D.J., Hull, P.M., Zelenitsky, D.K., Therrien, F., and Affek, H.P. (2020). Eggshell geochemistry reveals ancestral metabolic thermoregulation in Dinosauria. Sci. Adv. *6*, eaax9361. https://doi.org/10.1126/sciadv.aax9361.

14. Tagliavento, M., Davies, A.J., Bernecker, M., Staudigel, P.T., Dawson, R.R., Dietzel, M., Götschl, K., Guo, W., Schulp, A.S., Therrien, F., et al. (2023). Evidence for heterothermic endothermy and reptile-like eggshell mineralization in *Troodon*, a non-avian maniraptoran theropod. Proc. Natl. Acad. Sci. USA *120*, e2213987120. https://doi.org/10.1073/pnas.2213987120.

15. Wiemann, J., Menéndez, I., Crawford, J.M., Fabbri, M., Gauthier, J.A., Hull, P.M., Norell, M.A., and Briggs, D.E.G. (2022). Fossil biomolecules reveal an avian metabolism in the ancestral dinosaur. Nature *606*, 522–526. https://doi.org/10.1038/s41586-022-04770-6.

16. Barrett, P.M., Evans, D.C., and Campione, N.E. (2015). Evolution of dinosaur epidermal structures. Biol. Lett. *11*, 20150229. https://doi.org/10.1098/rsbl.2015.0229.

17. Motani, R., Gold, D.A., Carlson, S.J., and Vermeij, G.J. (2023). Amniote metabolism and the evolution of endothermy. Nature *621*, E1–E3. https://doi.org/10.1038/s41586-023-06411-y.

18. Grady, J.M., Enquist, B.J., Dettweiler-Robinson, E., Wright, N.A., and Smith, F.A. (2014). Dinosaur physiology. Evidence for mesothermy in dinosaurs. Science *344*, 1268–1272. https://doi.org/10.1126/science.1253143.

19. Benton, M.J. (2021). The origin of endothermy in synapsids and archosaurs and arms races in the Triassic. Gondwana Res. *100*, 261–289. https://doi.org/10.1016/j.gr.2020.08.003.

20. Santini, L., Isaac, N.J.B., Maiorano, L., Ficetola, G.F., Huijbregts, M.A.J., Carbone, C., and Thuiller, W. (2018). Global drivers of population density in terrestrial vertebrates. Global Ecol. Biogeogr. *27*, 968–979. https://doi.org/10.1111/geb.12758.

21. Chiarenza, A.A., Waterson, A.M., Schmidt, D.N., Valdes, P.J., Yesson, C., Holroyd, P.A., Collinson, M.E., Farnsworth, A., Nicholson, D.B., Varela, S., and Barrett, P.M. (2023). 100 million years of turtle paleoniche dynamics enable the prediction of latitudinal range shifts in a warming world. Curr. Biol. *33*, 109–121.e3. https://doi.org/10.1016/j.cub.2022.11.056.

22. Bell, P.R., Campione, N.E., Persons, W.S., Currie, P.J., Larson, P.L., Tanke, D.H., and Bakker, R.T. (2017). Tyrannosauroid integument reveals conflicting patterns of gigantism and feather evolution. Biol. Lett. *13*, 20170092. https://doi.org/10.1098/rsbl.2017.0092.

23. Rezende, E.L., Bacigalupe, L.D., Nespolo, R.F., and Bozinovic, F. (2020). Shrinking dinosaurs and the evolution of endothermy in birds. Sci. Adv. *6*, eaaw4486. https://doi.org/10.1126/sciadv.aaw4486.

24. Simpson, G.G. (1944). Tempo and Mode in Evolution (Columbia University Press).

25. Padian, K., and Horner, J. (2004). Dinosauria physiology. In The Dinosauria, Second Edition, D.B. Weishampel, P. Dodson, and H. Osmólska, eds. (University of California Press), pp. 660–671. https://doi.org/10.1525/9780520941434-035.

26. Haywood, A.M., Valdes, P.J., Aze, T., Barlow, N., Burke, A., Dolan, A.M., von der Heydt, A.S., Hill, D.J., Jamieson, S.S.R., Otto-Bliesner, B.L., et al. (2019). What can Palaeoclimate Modelling do for you? Earth Syst. Environ. *3*, 1–18. https://doi.org/10.1007/s41748-019-00093-1.

27. Felsenstein, J. (1985). Phylogenies and the comparative method. Am. Nat. *125*, 1–15. https://doi.org/10.1086/284325.

28. Hansen, T.F. (1997). Stabilizing selection and the comparative analysis of adaptation. Evolution *51*, 1341–1351. https://doi.org/10.1111/j.1558-5646.1997.tb01457.x.

29. Beaulieu, J.M., Jhwueng, D.-C., Boettiger, C., and O'Meara, B.C. (2012). Modeling stabilizing selection: expanding the Ornstein–Uhlenbeck model of adaptive evolution. Evolution *66*, 2369–2383. https://doi.org/10.1111/j.1558-5646.2012.01619.x.

30. Hansen, T.F. (2013). Adaptive Landscapes and Macroevolutionary Dynamics (Oxford University Press).

31. Paul, G.S., and Larramendi, A. (2023). Body mass estimate of *Bruhathkayosaurus* and other fragmentary sauropod remains suggest the largest land animals were about as big as the greatest whales. Lethaia *56*, 1–11. https://doi.org/10.18261/let.56.2.5.

32. Mannion, P.D., Benson, R.B.J., Upchurch, P., Butler, R.J., Carrano, M.T., and Barrett, P.M. (2012). A temperate palaeodiversity peak in Mesozoic dinosaurs and evidence for Late Cretaceous geographical partitioning. Glob. Ecol. Biogeogr. *21*, 898–908. https://doi.org/10.1111/j.1466-8238.2011.00735.x.

33. Rubel, F., and Kottek, M. (2011). Comments on: "The thermal zones of the Earth" by Wladimir Köppen (1884). Meteorol. Z. *20*, 361–365. https://doi.org/10.1127/0941-2948/2011/0285.

34. Galván, S., Gamboa, S., and Varela, S. (2023). Köppen Geiger Climatic Classification for R Users. Preprint at EarthArXiv. https://doi.org/10.31223/X5839B.

35. Burgener, L., Hyland, E., Reich, B.J., and Scotese, C. (2023). Cretaceous climates: mapping paleo-Köppen climatic zones using a Bayesian statistical analysis of lithologic, paleontologic, and geochemical proxies. Palaeogeogr. Palaeoclimatol. Palaeoecol. *613*, 111373. https://doi.org/10.1016/j.palaeo.2022.111373.

36. Noto, C.R., and Grossman, A. (2010). Broad-scale patterns of Late Jurassic dinosaur paleoecology. PLOS ONE *5*, e12553. https://doi.org/10.1371/journal.pone.0012553.

37. Coria, R.A., and Currie, P.J. (2006). A new carcharodontosaurid (Dinosauria, Theropoda) from the Upper Cretaceous of Argentina. Geodiversitas *28*, 71–118. https://sciencepress.mnhn.fr/en/periodiques/geodiversitas/28/1/un-nouveau-carcharodontosauride-dinosauria-theropoda-du-cretace-superieur-d-argentine.

38. Mannion, P.D., and Upchurch, P. (2010). A quantitative analysis of environmental associations in sauropod dinosaurs. Paleobiology *36*, 253–282. https://doi.org/10.1666/08085.1.

39. Mannion, P.D., and Upchurch, P. (2010). Completeness metrics and the quality of the sauropodomorph fossil record through geological and historical time. Paleobiology *36*, 283–302. https://doi.org/10.1666/09008.1.

40. Beerling, D.J., and Osborne, C.P. (2002). Physiological ecology of Mesozoic polar forests in a high CO_2 environment. Ann. Bot. *89*, 329–339. https://doi.org/10.1093/aob/mcf045.

41. Brentnall, S.J., Beerling, D.J., Osborne, C.P., Harland, M., Francis, J.E., Valdes, P.J., and Wittig, V.E. (2005). Climatic and ecological determinants of leaf lifespan in polar forests of the high CO2 Cretaceous 'greenhouse' world. Global Change Biol. *11*, 2177–2195. https://doi.org/10.1111/j.1365-2486.2005.001068.x.

42. Peralta-Medina, E., and Falcon-Lang, H.J. (2012). Cretaceous forest composition and productivity inferred from a global fossil wood database. Geology *40*, 219–222. https://doi.org/10.1130/G32733.1.

43. Fiorillo, A.R. (2017). Alaska Dinosaurs: An Ancient Arctic World (CRC Press). https://doi.org/10.1201/b22215.

44. Falcon-Lang, H.J., and Cantrill, D.J. (2001). Leaf phenology of some mid-Cretaceous polar forests, Alexander Island, Antarctica. Geol. Mag. *138*, 39–52. https://doi.org/10.1017/S0016756801004927.

45. Spicer, R.A., Rees, P., Chapman, J.L., Jarzembowski, E.A., Cantrill, D., Allen, J.R.L., Hoskins, B.J., Sellwood, B.W., Spicer, R.A., and Valdes, P.J. (1993). Cretaceous phytogeography and climate signals. Phil. Trans. R. Soc. Lond. B *341*, 277–286. https://doi.org/10.1098/rstb.1993.0113.

46. Poropat, S.F., Mannion, P.D., Upchurch, P., Hocknull, S.A., Kear, B.P., Kundrát, M., Tischler, T.R., Sloan, T., Sinapius, G.H.K., Elliott, J.A., and Elliott, D.A. (2016). New Australian sauropods shed light on Cretaceous

dinosaur palaeobiogeography. Sci. Rep. *6*, 34467. https://doi.org/10.1038/srep34467.

47. Averianov, A.O., Skutschas, P.P., Schellhorn, R., Lopatin, A.V., Kolosov, P.N., Kolchanov, V.V., Vitenko, D.D., Grigoriev, D.V., and Martin, T. (2020). The northernmost sauropod record in the Northern Hemisphere. Lethaia *53*, 362–368. https://doi.org/10.1111/let.12362.
48. Xuri, W., Hailu, Y., Qingjin, M., Chunling, G., Xiaodong, C., and Jinyuan, L. (2007). *Dongbeititan dongi*, the first sauropod dinosaur from the Lower Cretaceous Jehol Group of Western Liaoning Province, China. Acta Geologica Sinica (Eng) *81*, 911–916. https://doi.org/10.1111/j.1755-6724.2007.tb01013.x.
49. Zhonghe, Z. (2006). Evolutionary radiation of the Jehol Biota: chronological and ecological perspectives. Geol. J. *41*, 377–393. https://doi.org/10.1002/gj.1045.
50. Upchurch, P. (1995). The evolutionary history of sauropod dinosaurs. Phil. Trans. R. Soc. Lond. B *349*, 365–390. https://doi.org/10.1098/rstb.1995.0125.
51. Coria, R.A., Moly, J.J., Reguero, M., Santillana, S., and Marenssi, S. (2013). A new ornithopod (Dinosauria; Ornithischia) from Antarctica. Cret. Res. *41*, 186–193. https://doi.org/10.1016/j.cretres.2012.12.004.
52. Rauhut, O.W.M., and Pol, D. (2019). Probable basal allosauroid from the early Middle Jurassic Cañadón Asfalto Formation of Argentina highlights phylogenetic uncertainty in tetanuran theropod dinosaurs. Sci. Rep. *9*, 18826. https://doi.org/10.1038/s41598-019-53672-7.
53. Lee, M.S.Y., Cau, A., Naish, D., and Dyke, G.J. (2014). Dinosaur evolution. Sustained miniaturization and anatomical innovation in the dinosaurian ancestors of birds. Science *345*, 562–566. https://doi.org/10.1126/science.1252243.
54. Xu, X., Zhou, Z., Dudley, R., Mackem, S., Chuong, C.-M., Erickson, G.M., and Varricchio, D.J. (2014). An integrative approach to understanding bird origins. Science *346*, 1253293. https://doi.org/10.1126/science.1253293.
55. Cau, A. (2018). The assembly of the avian body plan: a 160-million-year long process. Boll. Soc. Paleontol. Ital. *57*, 1–25. https://doi.org/10.4435/BSPI.2018.01.
56. Huber, B.T., MacLeod, K.G., Watkins, D.K., and Coffin, M.F. (2018). The rise and fall of the Cretaceous Hot Greenhouse climate. Glob. Planet. Change *167*, 1–23. https://doi.org/10.1016/j.gloplacha.2018.04.004.
57. Reolid, M., Ruebsam, W., and Benton, M.J. (2022). Impact of the Jenkyns Event (early Toarcian) on dinosaurs: Comparison with the Triassic/Jurassic transition. Earth Sci. Rev. *234*, 104196. https://doi.org/10.1016/j.earscirev.2022.104196.
58. Pol, D., Ramezani, J., Gomez, K., Carballido, J.L., Carabajal, A.P., Rauhut, O.W.M., Escapa, I.H., and Cúneo, N.R. (2020). Extinction of herbivorous dinosaurs linked to Early Jurassic global warming event. Proc. Biol. Sci. *287*, 20202310. https://doi.org/10.1098/rspb.2020.2310.
59. Griffin, C.T., and Nesbitt, S.J. (2020). Does the maximum body size of theropods increase across the Triassic–Jurassic boundary? Integrating Ontogeny, Phylogeny, and Body Size. Anat. Rec. (Hoboken) *303*, 1158–1169. https://doi.org/10.1002/ar.24130.
60. Dunne, E.M., Farnsworth, A., Benson, R.B.J., Godoy, P.L., Greene, S.E., Valdes, P.J., Lunt, D.J., and Butler, R.J. (2023). Climatic controls on the ecological ascendancy of dinosaurs. Curr. Biol. *33*, 206–214.e4. https://doi.org/10.1016/j.cub.2022.11.064.
61. Godefroit, P., Sinitsa, S.M., Dhouailly, D., Bolotsky, Y.L., Sizov, A.V., McNamara, M.E., Benton, M.J., and Spagna, P. (2014). Dinosaur evolution. A Jurassic ornithischian dinosaur from Siberia with both feathers and scales. Science *345*, 451–455. https://doi.org/10.1126/science.1253351.
62. Bourke, J.M., Porter, W.R., and Witmer, L.M. (2018). Convoluted nasal passages function as efficient heat exchangers in ankylosaurs (Dinosauria: Ornithischia: Thyreophora). PLOS ONE *13*, e0207381. https://doi.org/10.1371/journal.pone.0207381.
63. Radermacher, V.J., Fernandez, V., Schachner, E.R., Butler, R.J., Bordy, E.M., Naylor Hudgins, M., de Klerk, W.J., Chapelle, K.E., and Choiniere, J.N. (2021). A new *Heterodontosaurus* specimen elucidates the unique ventilatory macroevolution of ornithischian dinosaurs. eLife *10*, e66036. https://doi.org/10.7554/eLife.66036.
64. Chiarenza, A.A., Fabbri, M., Consorti, L., Muscioni, M., Evans, D.C., Cantalapiedra, J.L., and Fanti, F. (2021). An Italian dinosaur Lagerstätte reveals the tempo and mode of hadrosauriform body size evolution. Sci. Rep. *11*, 23295. https://doi.org/10.1038/s41598-021-02490-x.
65. Zanno, L.E., and Makovicky, P.J. (2013). Neovenatorid theropods are apex predators in the Late Cretaceous of North America. Nat. Commun. *4*, 2827. https://doi.org/10.1038/ncomms3827.
66. Sues, H.-D., and Averianov, A. (2009). A new basal hadrosauroid dinosaur from the Late Cretaceous of Uzbekistan and the early radiation of duck-billed dinosaurs. Proc. Biol. Sci. *276*, 2549–2555. https://doi.org/10.1098/rspb.2009.0229.
67. Prieto-Márquez, A. (2010). Global historical biogeography of hadrosaurid dinosaurs. Zool. J. Linn. Soc. *159*, 503–525. https://doi.org/10.1111/j.1096-3642.2010.00642.x.
68. Grellet-Tinner, G., and Fiorelli, L.E. (2010). A new Argentinean nesting site showing neosauropod dinosaur reproduction in a Cretaceous hydrothermal environment. Nat. Commun. *1*, 32. https://doi.org/10.1038/ncomms1031.
69. Henderson, D.M. (2013). Sauropod necks: are they really for heat loss? PLOS ONE *8*, e77108. https://doi.org/10.1371/journal.pone.0077108.
70. Wedel, M.J. (2005). Postcranial skeletal pneumaticity in sauropods and its implications for mass estimates. In The Sauropods: Evolution and Paleobiology, K.C. Rogers, ed. (University of California Press), pp. 201–228. https://doi.org/10.1525/california/9780520246232.003.0008.
71. Sander, P.M. (2013). An evolutionary cascade model for sauropod dinosaur gigantism - overview, update and tests. PLOS ONE *8*, e78573. https://doi.org/10.1371/journal.pone.0078573.
72. Benson, R.B.J., Hunt, G., Carrano, M.T., and Campione, N. (2018). Cope's rule and the adaptive landscape of dinosaur body size evolution. Palaeontology *61*, 13–48. https://doi.org/10.1111/pala.12329.
73. Ding, A., Pittman, M., Upchurch, P., O'Connor, J., Field, D.J., and Xu, X. (2019). The biogeography of coelurosaurian theropods and its impact on their evolutionary history. In Pennaraptoran Theropod Dinosaurs: Past Progress and New Frontiers (American Museum of Natural History), pp. 117–157. https://doi.org/10.1101/634170.
74. Benson, R.B.J., Campione, N.E., Carrano, M.T., Mannion, P.D., Sullivan, C., Upchurch, P., and Evans, D.C. (2014). Rates of dinosaur body mass evolution indicate 170 million years of sustained ecological innovation on the avian stem lineage. PLOS Biol. *12*, e1001853. https://doi.org/10.1371/journal.pbio.1001853.
75. Gould, S.J., and Vrba, E.S. (1982). Exaptation—a missing term in the science of form. Paleobiology *8*, 4–15. https://doi.org/10.1017/S0094837300004310.
76. Barta, D.E., Griffin, C.T., and Norell, M.A. (2022). Osteohistology of a Triassic dinosaur population reveals highly variable growth trajectories typified early dinosaur ontogeny. Sci. Rep. *12*, 17321. https://doi.org/10.1038/s41598-022-22216-x.
77. Seebacher, F. (2020). Is endothermy an evolutionary by-product? Trends Ecol. Evol. *35*, 503–511. https://doi.org/10.1016/j.tree.2020.02.006.
78. Tennant, J.P., Chiarenza, A.A., and Baron, M. (2018). How has our knowledge of dinosaur diversity through geologic time changed through research history? PeerJ *6*, e4417. https://doi.org/10.7717/peerj.4417.
79. Scotese, C., Wright, N., and Paleo, D.E.M. (2018). Resource – Scotese and Wright. EarthByte.
80. Jones, L.A., Gearty, W., Allen, B.J., Eichenseer, K., Dean, C.D., Galván, S., Kouvari, M., Godoy, P.L., Nicholl, C.S.C., Buffan, L., et al. (2023). palaeoverse: A community-driven R package to support palaeobiological analysis. Methods Ecol. Evol. *14*, 2205–2215. https://doi.org/10.1111/2041-210X.14099.

81. Lloyd, G.T., Bapst, D.W., Friedman, M., and Davis, K.E. (2016). Probabilistic divergence time estimation without branch lengths: dating the origins of dinosaurs, avian flight and crown birds. Biol. Lett. *12*, 20160609. https://doi.org/10.1098/rsbl.2016.0609.

82. Hedman, M.M. (2010). Constraints on clade ages from fossil outgroups. Paleobiology *36*, 16–31. https://doi.org/10.1666/0094-8373-36.1.16.

83. Valdes, P.J., Armstrong, E., Badger, M.P.S., Bradshaw, C.D., Bragg, F., Davies-Barnard, T., Day, J.J., Farnsworth, A., Hopcroft, P.O., Kennedy, A.T., et al. (2017). The BRIDGE HadCM3 family of climate models:HadCM3@Bristol v1.0. Geosci. Model Dev. *10*, 3715–3743. https://doi.org/10.5194/gmd-2017-16.

84. Valdes, P.J., Scotese, C.R., and Lunt, D.J. (2021). Deep ocean temperatures through time. Clim. Past *17*, 1483–1506. https://doi.org/10.5194/cp-17-1483-2021.

85. Sagoo, N., Valdes, P., Flecker, R., and Gregoire, L.J. (2013). The Early Eocene equable climate problem: can perturbations of climate model parameters identify possible solutions? Philos. Trans. A Math. Phys. Eng. Sci. *371*, 20130123. https://doi.org/10.1098/rsta.2013.0123.

86. Kiehl, J.T., and Shields, C.A. (2013). Sensitivity of the Palaeocene–Eocene thermal maximum climate to cloud properties. Philos. Trans. A Math. Phys. Eng. Sci. *371*, 20130093. https://doi.org/10.1098/rsta.2013.0093.

87. Cox, M.D. (1984). A Primitive Equation, 3-Dimensional Model of the Ocean. In GFDL Ocean Group Technical Report No. 1 (Geophysical Fluid Dynamics Laboratory).

88. Lunt, D.J., Farnsworth, A., Loptson, C., Foster, G.L., Markwick, P., O'Brien, C.L., Pancost, R.D., Robinson, S.A., and Wrobel, N. (2016). Palaeogeographic controls on climate and proxy interpretation. Clim. Past *12*, 1181–1198. https://doi.org/10.5194/cp-12-1181-2016.

89. Valdes, P.J., Armstrong, E., Badger, M.P.S., Bradshaw, C.D., Bragg, F., Crucifix, M., Davies-Barnard, T., Day, J.J., Farnsworth, A., Gordon, C., et al. (2017). The BRIDGE HadCM3 family of climate models: HadCM3@Bristol v1.0. Geosci. Model Dev. *10*, 3715–3743. https://doi.org/10.5194/gmd-10-3715-2017.

90. Farnsworth, A., Lunt, D.J., O'Brien, C.L., Foster, G.L., Inglis, G.N., Markwick, P., Pancost, R.D., and Robinson, S.A. (2019). Climate sensitivity on geological timescales controlled by nonlinear feedbacks and ocean circulation. Geophys. Res. Lett. *46*, 9880–9889. https://doi.org/10.1029/2019GL083574.

91. Chiarenza, A.A., Farnsworth, A., Mannion, P.D., Lunt, D.J., Valdes, P.J., Morgan, J.V., and Allison, P.A. (2020). Asteroid impact, not volcanism, caused the end-Cretaceous dinosaur extinction. Proc. Natl. Acad. Sci. USA *117*, 17084–17093. https://doi.org/10.1073/pnas.2006087117.

92. Chiarenza, A.A., Mannion, P.D., Lunt, D.J., Farnsworth, A., Jones, L.A., Kelland, S.-J., and Allison, P.A. (2019). Ecological niche modelling does not support climatically-driven dinosaur diversity decline before the Cretaceous/Paleogene mass extinction. Nat. Commun. *10*, 1091. https://doi.org/10.1038/s41467-019-08997-2.

93. Chiarenza, A. (2019). Virtual habitats, fossil preservation, and estimates of dinosaur biodiversity in the Cretaceous of North America. PhD thesis (Cambridge University)). https://doi.org/10.25560/93884.

94. Dunne, E.M., Farnsworth, A., Greene, S.E., Lunt, D.J., and Butler, R.J. (2021). Climatic drivers of latitudinal variation in Late Triassic tetrapod diversity. Palaeontology *64*, 101–117. https://doi.org/10.1111/pala.12514.

95. García-Girón, J., Heino, J., Alahuhta, J., Chiarenza, A.A., and Brusatte, S.L. (2021). Palaeontology meets metacommunity ecology: the Maastrichtian dinosaur fossil record of North America as a case study. Palaeontology *64*, 335–357. https://doi.org/10.1111/pala.12526.

96. Foster, G.L., Royer, D.L., and Lunt, D.J. (2017). Future climate forcing potentially without precedent in the last 420 million years. Nat. Commun. *8*, 14845. https://doi.org/10.1038/ncomms14845.

97. Gough, D.O. (1981). Solar interior structure and luminosity variations. Sol. Phys. *74*, 21–34. https://doi.org/10.1007/BF00151270.

98. Revell, L.J. (2009). Size-correction and principal components for interspecific comparative studies. Evolution *63*, 3258–3268. https://doi.org/10.1111/j.1558-5646.2009.00804.x.

99. Pagel, M. (1999). Inferring the historical patterns of biological evolution. Nature *401*, 877–884. https://doi.org/10.1038/44766.

100. Revell, L.J. (2012). phytools: an R package for phylogenetic comparative biology (and other things). Methods Ecol. Evol. *3*, 217–223. https://doi.org/10.1111/j.2041-210X.2011.00169.x.

101. Gates, T.A., Organ, C., and Zanno, L.E. (2016). Bony cranial ornamentation linked to rapid evolution of gigantic theropod dinosaurs. Nat. Commun. *7*, 12931. https://doi.org/10.1038/ncomms12931.

102. Pennell, M.W., Eastman, J.M., Slater, G.J., Brown, J.W., Uyeda, J.C., FitzJohn, R.G., Alfaro, M.E., and Harmon, L.J. (2014). geiger v2.0: an expanded suite of methods for fitting macroevolutionary models to phylogenetic trees. Bioinformatics *30*, 2216–2218. https://doi.org/10.1093/bioinformatics/btu181.

103. Sereno, P.C. (1998). A rationale for phylogenetic definitions, with application to the higher-level taxonomy of Dinosauria [41–83. N. Jahrb. Geol. Paläontol. Abh. *210*, 41–83. https://doi.org/10.1127/njgpa/210/1998/41.

104. Madzia, D., Arbour, V.M., Boyd, C.A., Farke, A.A., Cruzado-Caballero, P., and Evans, D.C. (2021). The phylogenetic nomenclature of ornithischian dinosaurs. PeerJ *9*, e12362. https://doi.org/10.7717/peerj.12362.

105. Nopcsa, F. (1915). Die Dinosaurier der siebenbürgischen Landesteile Ungarns: Von Franz Baron Nopcsa. Mit Tafel I - IV und 3 Figuren im Texte. [Umschlagtitel.] (Buchdruckerei des Franklin-Vereins).

106. Cooper, M.R. (1985). A revision of the ornithischian dinosaur *Kangnasaurus coetzeei* Haughton, with a classification of the Ornithischia. Ann. S. Afr. Mus. *95*, 281–317. https://biostor.org/reference/109745.

107. Bonaparte, J.F. (1986). The early radiation and phylogenetic relationships of Jurasic sauropod dinosaurs, based on vertebral anatomy. In The Beginning of the Age of Dinosaurs, K. Padian, ed. (Cambridge University Press), pp. 247–258.

108. Wilson, J.A., and Sereno, P.C. (1998). Early evolution and higher-level phylogeny of sauropod dinosaurs. Journal of Vertebrate Paleontology *18*, 1–79. https://doi.org/10.1080/02724634.1998.10011115.

109. Mannion, P.D., Upchurch, P., Barnes, R.N., and Mateus, O. (2013). Osteology of the Late Jurassic Portuguese sauropod dinosaur *Lusotitan atalaiensis* (Macronaria) and the evolutionary history of basal titanosauriforms. Zool. J. Linn. Soc. *168*, 98–206. https://doi.org/10.1111/zoj.12029.

110. Gauthier, J. (1986). Saurischian monophyly and the origin of birds. Mem. Calif. Acad. Sci. *8*, 1–55. https://biostor.org/reference/110202.

111. Holtz, T.R. (1996). Phylogenetic taxonomy of the Coelurosauria (Dinosauria: Theropoda). J. Paleontol. *70*, 536–538. https://doi.org/10.1017/S0022336000038506.

112. Holtz, T., Molnar, R., and Currie, P. (2004). Basal Tetanurae. In The Dinosauria, Second Edition, D.B. Weishampel, P. Dodson, and H. Osmólska, eds. (University of California Press), pp. 71–110. https://doi.org/10.1525/california/9780520242098.003.0006.

113. Butler, M.A., and King, A.A. (2004). Phylogenetic comparative analysis: a modeling approach for adaptive evolution. Am. Nat. *164*, 683–695. https://doi.org/10.1086/426002.

114. Felsenstein, J. (1973). Maximum likelihood estimation of evolutionary trees from continuous characters. Am. J. Hum. Genet. *25*, 471–492.

115. Blomberg, S.P., Garland, T., and Ives, A.R. (2003). Testing for phylogenetic signal in comparative data: behavioral traits are more labile. Evolution *57*, 717–745. https://doi.org/10.1111/j.0014-3820.2003.tb00285.x.

116. Jin, X., Shi, Z., Baranyi, V., Kemp, D.B., Han, Z., Luo, G., Hu, J., He, F., Chen, L., and Preto, N. (2020). The Jenkyns Event (early Toarcian OAE) in the Ordos Basin, North China. Glob. Planet. Change *193*, 103273. https://doi.org/10.1016/j.gloplacha.2020.103273.

117. Tennant, J.P., Mannion, P.D., Upchurch, P., Sutton, M.D., and Price, G.D. (2017). Biotic and environmental dynamics through the Late Jurassic–Early Cretaceous transition: evidence for protracted faunal

and ecological turnover. Biol. Rev. Camb. Philos. Soc. *92*, 776–814. https://doi.org/10.1111/brv.12255.

118. Clarke, L.J., and Jenkyns, H.C. (1999). New oxygen isotope evidence for long-term Cretaceous climatic change in the Southern Hemisphere. Geology *27*, 699–702. https://doi.org/10.1130/0091-7613(1999)027<0699:NOIEFL>2.3.CO;2.

119. Beck, H.E., Zimmermann, N.E., McVicar, T.R., Vergopolan, N., Berg, A., and Wood, E.F. (2018). Present and future Köppen-Geiger climate classification maps at 1-km resolution. Sci. Data *5*, 180214. https://doi.org/10.1038/sdata.2018.214.

120. Hijmans, R.J., Bivand, R., Pebesma, E., and Sumner, M.D. (2023). Terra: Spatial Data Analysis. version 1, pp. 7–55.

121. Varela, S., and Rothkugel, S. (2018). mapast-R-package: mapast: MAp the PAST. in macroecology/paleoMap: Paleogeography Combined with Spatial Paleobiodiversity. https://rdrr.io/github/macroecology/paleoMap/man/mapast-R-package.html.

122. Scotese, C. (2016). PALEOMAP PaleoAtlas for GPlates and the PaleoData Plotter Program. https://doi.org/10.13140/RG.2.2.34367.00166.

123. Sugiura, N. (1978). Further analysts of the data by Akaike' s information criterion and the finite corrections: further analysts of the data by Akaike' s. Commun. Stat. Theor. Methods *7*, 13–26. https://doi.org/10.1080/03610927808827599.

124. Beaulieu, J.M., and O'Meara, B. (2022). OUwie: Analysis of Evolutionary Rates in an OU Framework. version 2.10.

125. Revell, L.J., and Harmon, L.J. (2022). Phylogenetic Comparative Methods in R (Princeton University Press).

STAR★METHODS

KEY RESOURCES TABLE

REAGENT OR RESOURCE	SOURCE	IDENTIFIER
Deposited data		
Dinosaur fossil occurrences, climate variables and phylogenetic trees used in this study	DOI: https://figshare.com/s/3144b9e4e16361d37404	Repository data files
Palaeoclimate models used in this study	DOI: https://www.paleo.bristol.ac.uk/ummodel/scripts/papers/?	files_Ale_Scot_Ind_Maa
Software and algorithms		
R package mapast V 0.1	https://rdrr.io/github/macroecology/paleoMap/man/mapast-R-package.html.	N/A
R package palaeoverse V 1.2.1	https://cran.r-project.org/package=palaeoverse	N/A
R package dismo V 1.3-5	https://cran.r-project.org/web/packages/dismo/index.html	N/A
R package stats V 4.2.0	https://stat.ethz.ch/R-manual/R-devel/library/stats/html/00Index.html	N/A
R package ggplot2 V 3.3.5	https://cran.r-project.org/web/packages/ggplot2/index.html	N/A
R package phytools V 1.9-16	https://cran.r-project.org/package=phytools	N/A
R package terra V 1.7-39	https://cran.r-project.org/package=terra	N/A
R package OUwie V 2.10	https://cran.r-project.org/package=OUwie	N/A
R package raster V 3.5-2	https://cran.r-project.org/web/packages/raster/index.html	N/A

RESOURCE AVAILABILITY

Lead contact

Further information and requests for resources and reagents should be directed to and will be fulfilled by the lead contact, Alfio Alessandro Chiarenza (a.chiarenza15@gmail.com).

Materials availability

This study did not generate new unique materials.

Data and code availability

Quantitative and statistical routines are reported in the STAR Methods. The fossil occurrence data, related climatic variables and phylogenetic trees used in this study are available as repository data file 1–4 under a CC BY 4.0 licence at this DOI: https://doi.org/10.6084/m9.figshare.24879003.v1. General Circulation Models and palaeoclimatic data used here come from the BRIDGE group and are available at: https://www.paleo.bristol.ac.uk/ummodel/scripts/papers/?). All other data are available in the main text, STAR Methods, or the supplemental information.

EXPERIMENTAL MODEL AND SUBJECT DETAILS

Fossil dataset

We developed a specimen-based occurrence dataset, building on previous efforts from Benson et al.[72] The occurrences were originally sourced from the Paleobiology Database (https://paleobiodb.org/#/) but required vetting to ensure that the relevant specimens were correctly anchored to the respective taxa used in the tree and along with the correct stratigraphic and geographic information (repository data file 1). We modified the dataset for a total of 993 occurrences, updating entries according to current taxonomic information and providing references for previously unavailable or ambiguous data (e.g., locality data). Palaeogeographic reconstructions were performed using the Global Plate Model PALEOMAP,[79] implemented via the 'palaeorotate' function in the R package palaeoverse ver. 1.2.1.[80]

Phylogenetic Data for macroevolutionary modelling

In this study, we focused on the largest phylogenetic analyses currently available, closer to the current consensus on in group relationships, and including as many taxonomic tips as possible for the three main dinosaur subclades: Ornithischia, Sauropodomorpha and Theropoda (repository data file 1). A phylogeny for each subclade was sourced from Benson et al.[72] (originally published by Benson et al.[74]). Notably, the theropod phylogeny from Benson et al.[72] included taxa from the Carnian stage of the Upper Triassic to the Aptian stage of the Lower Cretaceous. To compensate for the lack of post-Aptian theropods, and given our interest in exploring the trends in theropod climatic niche space up to the Cretaceous/Palaeogene boundary, we conducted macroevolutionary modelling analyses for Theropoda using the phylogeny published by Cau.[55] This latter, more complete phylogeny of Theropoda, is based on a phylogenetic data matrix including 1,781 morphological character statements for 132 operational taxonomic unit.[55] Given the original criteria for assembling this dataset included, beyond broad taxonomic sampling, preferring taxa with higher amount of skeletal completeness and more robustly placed positions related to the consensus expressed by other phylogenetic analyses,[55] the output tree from this matrix was preferred for phylogenetic comparative analyses rather than using a secondarily assembled, composite supertree.

The tree used for Sauropodomorpha[72] contains 98 tips, the tree for Ornithischia[72] contains 126 tips, while the tree for Theropoda[55] contains 132 tips (repository data file 1). In order to congruently fit the phylogenetic theropod tree tips with the available climatically calibrated fossil occurrences, 33 taxa were excluded from the analysis, rendering a final tree with 99 tips (repository data file 1). The tips dropped in the final tree from Cau[55] are: *Meleagris*, *Teleocrater, Euparkeria, Buriolestes, Sanjuansaurus, Chilesaurus, Bicentenaria, Gualicho, Jianchangosaurus, Halszkaraptor*, *Jianianhualong, Gobivenator, Anchiornis* (holotype), *Serikornis, Aurornis, Cruralispennia, Chongmingia, Zhouornis, Sulcavis, Bohaiornis, Parahongshanornis, Archaeornithura, Piscivoravis, Iteravis, Yi, Berberosaurus, Coelurus, Eodromaeus*, *Epidendrosaurus*, *Guaibasaurus*, *Shenzhouraptor*, *Sinocalliopteryx* and *Sinusonasus*.

To deal with phylogenetic uncertainty related to different topologies (due to slightly inconsistent inter-nodal relationships in each of the phylogenies of the selected subclades), we randomly chose one of the 20 trees in each tree object for the Benson et al. dataset.[72] The Cau[55] theropod tree used is the Maximum Clade Credibility Tree topology (MCCT) obtained as output of the Bayesian analyses (see details in Cau[55]). Time calibration for the Benson et al. dataset[72] was performed by assigning ages in each tip as the uniform distributions between the minimum (LAD) and maximum (FAD) possible ages for each taxon, with both FAD and LAD being scrutinized, vetted and updated for this study (see repository data file 1), and with node age calibration following the Lloyd et al.[81] modified probabilistic method by Hedman.[82] These trees[72] were calibrated with their roots at 239.7856 Ma while the more inclusive, Cau[55] tree was calibrated with the root at 252 Ma.

Palaeoclimate model

The global palaeoclimatic and land-surface model outputs used in this study spans from the Late Triassic (Carnian) to the end-Cretaceous (Maastrichtian). These data were produced from an updated version of the fully coupled Atmosphere-Ocean General Circulation Model (AOGCM) HadCM3, specifically, HadCM3L-M2.1D, following the nomenclature of Valdes et al.,[83] developed by the BRIDGE Group (http://www.bridge.bris.ac.uk/resources/simulations). This model has a critical update that includes modification to cloud condensation nuclei density and cloud droplet effective radius following recent work.[84–86] This raises higher latitude temperatures without significantly changing tropical temperatures reducing the pole-to-equator temperature gradient in line with proxy observations, a persistent problem that has afflicted many palaeoclimate models for decades. This update is also found to work under hot, cool, and icehouse climatic conditions, as well as under pre-industrial boundary conditions making it appropriate for use across modern and deep time evolving conditions.

Variables outputs from the General Circulation Model (GCM; experiment series teye[84]) used here include near-surface (1.5 m) mean annual temperature (ºC), near-surface (1.5 m) mean annual temperature standard deviation (ºC), mean annual average precipitation (mm), mean annual precipitation standard deviation (mm), net primary productivity (NPP, g C m-2 yr-1), and five plant functional types (broadleaf trees, deciduous trees, shrubs, C3-type and C4-type grasses) using an interactive vegetation scheme called TRIFFID (Top-Down Representation of Interactive Foliage and Flora Including Dynamics) using the MOSES 2.1 land surface scheme at a spatial resolution of 2.75º×3.25º latitude by longitude 278 km by 417 km grid square at the Equator). There are 19 hybrid levels in the atmosphere and 20 vertical levels in the ocean with equations solved on the Arakawa B-grid. As is common in all climate models, sub-grid scale processes such as cloud, convection and oceanic eddies are parameterized as they cannot be resolved at the scales required (usually meters to several kilometers) of the model resolution. The ocean model is based on the model of Cox et al.[87] and is a full primitive equation, three-dimensional model of the ocean.

The model simulations were conducted in a similar vein as comprehensively described in Lunt et al.,[88] Valdes et al.,[89] and Farnsworth et al.[90] The implications of deep-time studies of these GCM constraints were discussed in previous studies.[12,21,91–93] In summary, the model simulations ran for at least 6,000 (often many thousands of years more) model years until they reached full equilibrium in both the atmosphere and deep ocean. Equilibrium is determined by passing three criteria: i) the globally and volume-integrated annual mean ocean temperature trend is less than 1°C per 1,000 years; ii) trends in surface air temperature are less than 0.3°C per 1,000 years and; iii) net energy balance at the top of the atmosphere, averaged over a 100-year period at the end of the simulation, is less than 0.25/W m^2. The variables used in our study represent an annual average of the final 100 years of these simulations. Notably, these models captured temporal fluctuations, regional nuances, and large-scale circulations, including associated energy and momentum fluxes.[88] Despite the inherent uncertainty in the data, these models effectively replicated the modern-day climates of most terrestrial biomes.[89] Importantly, HadCM3L played a pivotal role in the Coupled Model Intercomparison Project experiments

and demonstrated its utility in various Mesozoic palaeobiogeographical investigations.[12,21,91,92,94] The palaeogeographic data employed in this study were derived from the dataset created by Scotese & Wright.[79] Originally conceived as a palaeo-digital elevation model (DEM) with a 1°×1° grid, these data were upscaled to match the resolution of the HadCM3L Earth System model (2.75°×3.25°). This upscaling process ensured that the topographic and bathymetric information was broadly preserved, despite its resolution being lowered.[12,91,95] These 117 palaeogeographic maps (covering the whole of the Phanerozoic) have served as a global atlas, facilitating regional-scale interpretations of palaeogeography over the past 540 million years, thereby elucidating the shifting distributions of Earth's oceans and continents. Here we focus only on 252 to 66 million years ago. Additional information regarding these datasets can be freely accessed at https://www.earthbyte.org/. Land ice was not included within the Scotese palaeogeography and is instead transformed onto the model grid assuming a simple parabolic shape to estimate the ice sheet height (m). Please see Valdes et al.[84] for further details. 'Realistic' pCO_2 concentrations for each simulation are based on Foster et al.[96] (Figure S1). Time specific solar luminosity for each simulation was based on Gough.[97]

METHOD DETAILS

Phylogenetic Principal Component Analyses

To evaluate climatic niche space occupation in a multivariate setting (combining several variables, like temperature and precipitation) we used Phylogenetic Principal Component Analyses (phyloPCA), which takes the non-independence between related species when computing covariates compared to a classic PCA.[98] First, we checked for collinearity of variables between all the physical outputs of the GCM, including seasonal and monthly temperature and precipitation values, and retaining those variables demonstrating a Pearson's correlation coefficient <0.7 (repository data file 4). The variables retained for the final phyloPCA included maximum mean annual temperature, minimum mean annual temperature, minimum mean annual precipitation, and precipitation seasonality. As a phylogenetic framework, we used an updated composite supertree for all Dinosauria (repository data file 1) from Benson et al.[72,74] which contains 642 tips of non-dinosaurian Dinosauromorpha and the three Dinosauria subclades (Ornithischia, Sauropodomorpha and Theropoda). To maximize phylogenetic control (i.e. controlling for phylogenetic signal) in the structure of the variance in our Principal Components, we used an optimized Pagel's λ[99] transformation. The object scores of the two main PCA axes (PC1 and PC2) were then extracted (repository data file 1) and used to model the occupation in multidimensional climatic niche space (see Macroevolutionary OU modelling section below). We used the R package phytools v.1.9-16[100] for phyloPCA analysis and plotting.

Ancestral State Reconstruction

We performed ancestral state reconstruction to map the evolution of physical environmental parameters, such as temperature, precipitation, and principal components derived from multidimensional climatic space (from phyloPCA, see Phylogenetic Principal Component Analyses section), treating them as continuous characters. We used the R package phytools v.1.9-16[100] to create a stochastic map with 10,000 generations, applying the 'SYM' (Symmetrical) model of evolution on the randomly selected, time-scaled consensus tree, following the approach by Gates et al.[101] as used in Chiarenza et al.[64] to reconstruct body-size evolution in ornithischian dinosaurs. The resulting ancestral state reconstruction was visualized as a density map on the phylogenetic trees for each dinosaur subclades (repository data file 3). Furthermore, we utilized a GEIGER-fitted comparative model for continuous data[102] to reconstruct the ancestral state (z_0 or root value) at the base of various dinosaur subclades Figure 2. For Ornithischia, ancestral states were reconstructed at the tree root (*Staurikosaurus*+*Fruitadens haagarorum*), for Thyreophora[103–105] (*Scutellosaurus* lawleri+*Edmontonia*), and for Neornithischia[103,104,106] (*Stormbergia* dangershoeki+*Corythosaurus*). Ancestral States Reconstructions (ASRs) were produced for Sauropodomorpha at the tree root (*Pisanosaurus*+*Chuanjiesaurus*), for non-somphospondylian Neosauropoda[50,107] (*Ferganasaurus*+*Giraffatitan*), and for Somphospondyli[108,109] (*Euhelopus*+*Saltasaurus*). ASRs were computed for Theropoda,[55] testing two different sets of ASR partitions: one (RTC) at the root of the tree including non-theropod dinosauromorphs (*Marasuchus*+*Heterodontosaurus*), non-coelurosaurian Theropoda[103,110] (*Dilophosaurus*+*Acrocanthosaurus*), and Coelurosauria[110] (*Zuolong*+*Vegavis*); the other regime partition (RCA) included the root of the tree with non-coelurosaurian dinosauromorphs (*Marasuchus*+*Acrocanthosaurus*), for non-avialan Coelurosauria[110–112] (*Zuolong*+*Mei*), and for Avialae[110] (*Anchiornis*+*Vegavis*).

Macroevolutionary OU modelling

We explored the evolution of the climatic landscape (niche space) of each dinosaur subgroup by means of Ornstein-Uhlenbeck (OU) dynamics.[28,29,113] Using this approach, we aimed to test the congruence of dinosaurian climatic landscape exploration against several constrained and well-documented evolutionary scenarios (like Brownian motion,[114] Early burst,[115] and multi-peak OU[28] models of evolution).

To accomplish this, we initially calibrated the phylogenetic tree with co-occurring climatic variables for the specimen-based tips (OTUs, Operation Taxonomic Units). Subsequently, we performed macroevolutionary modelling using OU models to investigate whether the evolution of each specific climatic trait value followed a stochastic diffusion pattern over time (like in a Brownian motion[114] scenario) or a directional, trend-like occupation (OU models) of climatic niche space. Given the predominance of temperature in explaining the variance of the data (see Phylogenetic Principal Component Analyses Methods section in STAR Methods and Figure 1), and the higher reliability (higher 'realism') of temperature as a GCM output compared to precipitation variables,[90] we further discussed and plotted only temperature related macroevolutionary models in the main results. We assessed whether each phylogenetic model followed any direction trend toward a macroevolutionary trait optimum (θ) at a given rate of variance accumulation (σ),

with a defined strength of attraction (α) at a particular phylogenetic node (OU model), at multiple nodes (OUM multiple regimes[28,29,113]) or under different time-partitions (repository data file 3). Temporal partitions (repository data file 2) for each tree were performed at the Jenkyns event[57,116] (early Toarcian, 183.0 Ma), at the Jurassic/Cretaceous boundary[117] (145.0 Ma) and at the Cenomanian/Turonian boundary[56,118] (93.9 Ma).

Climatic zones

Using our HadCM3L palaeoclimatic simulations (see related 'Palaeoclimate model' section above), we classified palaeogeographic landscapes into broad climatic zones following an adapted version of Köppen's climate classification. Retaining temperature and precipitation monthly data per time step (formatted as two arrays of twelve matrices, respectively), we implemented[34] the Köppen-Geiger[33] climate classification from Beck et al.[119] To do so, we used the provided function written in MATLAB (https://doi.org/10.6084/m9.figshare.6396959) to classify these climate data into five main climate classes: tropical, arid, temperate, cold, and polar. We introduced two changes to the original Beck et al.[119] function: i) we added a ''-99'' value for the missing values, in order to facilitate computational operations, and ii) we modified lines 84, 85 and 86 of KoppenGeiger.m in order to fulfil the following conditions: ''Pthreshold=2×MAT if >70% of precipitation falls in winter, Pthreshold=2×MAT+28 if >70% of precipitation falls in summer, otherwise defined as Pthreshold=2×MAT+14'' (H. Beck, personal communication, December 18, 2021). Once we have obtained the classified matrices per time step, we rasterized and rotated the resulting maps using the 'rast' and 'rotate' functions from the terra package version 1.7-39.[120]

We downloaded land configuration maps for all time periods using the 'getmap' function from the mapast package version 0.1,[121] using the PALEOMAP[122] reconstruction model as it is the same used as boundary conditions for our climate data. We cropped the previous reclassified maps with these palaeogeographic maps using the 'mask' function of the R package terra (version 1.7-39),[120] to retrieve land climatic zones' maps. Lastly, we used dinosaur palaeolatitude and palaeolongitude from our dataset (repository data file 1) to extract climatic zone information from each of the occurrences (repository data file 4). To do so, we used the 'extract' function of the terra version 1.7-39 package.[120] With this information, we calculated the number of dinosaur occurrences as percentages of total taxonomic diversity by subclade included in our trees (Ornithischia, Sauropodomorpha and Theropoda) and by climatic zone through time to obtain the quantification shown in Figure 3. Percentages are calculated in reference to the total number of occurrences for each time bin across climatic zones and clades. Values in the time series corresponding to bins with missing data are interpolated to bridge gaps between data-rich bins.

QUANTIFICATION AND STATISTICAL ANALYSIS

Phylogenetic comparative model performance evaluation

Phylogenetic model performance was compared (Table S1, repository data file 3) using the Akaike Information Criterion with finite correction,[123] excluding models that returned out of bounds (α, σ, θ) estimates. For the analysis of continuous trait evolution under selective regimes, we employed modified OU models,[28] using R version 4.3.0 and the OUwie package v.2.10[124] with codes from Revell and Harmon[125] (see also http://www.phytools.org/Rbook/).